Available online at www.sciencedirect.com
ScienceDirect
Dyes and Pigments 75 (2007) 533–543
DYES and PIGMENTS
www.elsevier.com/locate/dyepig

Photocatalytic degradation of azo dye (*Reactive Red 120*) in TiO_2/UV system: Optimization and modeling using a response surface methodology (RSM) based on the central composite design

Il-Hyoung Cho, Kyung-Duk Zoh*

Department of Environmental Health, Institute of Health & Environment, School of Public Health, Seoul National University, 28 Yunkeon, Jongro, Seoul 110-799, Korea

Received 24 November 2005; received in revised form 18 March 2006; accepted 28 June 2006
Available online 27 October 2006

Abstract

The aim of our research was to apply experimental design methodology in the optimization of photocatalytic degradation of azo dye (*Reactive Red 120*). The reactions were mathematically described as the function of parameters such as amount of TiO_2 (X_1), dye concentration (X_2) and UV intensity (X_3), and were modeled by the use of response surface methodology (RSM). These experiments were carried out as a central composite design (CCD) consisting of 20 experiments determined by the 2^3 full factorial designs with six axial points and six center points. The degradation of azo dye (*RR120*) followed an apparent first-order rate law in every pH condition. The results show that the responses of color removal (%) (Y_1) in photocatalysis of dyes were significantly affected by the synergistic effect of linear term of UV intensity (X_3) and the antagonistic effect of quadratic term of UV intensity (X_3^2). Significant factors and synergistic effects for the TOC removal (%) (Y_2) were the linear terms of TiO_2 (X_1), and UV intensity (X_3). However, the quadratic terms of TiO_2 (X_1^2) and UV intensity (X_3^2) had an antagonistic effect on Y_2 responses. Canonical analysis indicates that the stationary point was a saddle point for Y_1 response whereas a maximum point for Y_2 response. The estimated ridge of maximum responses and optimal conditions for Y_1 and Y_2 using canonical analysis were 100% and 67.27%, respectively. The experimental values agreed with the predicted ones, indicating suitability of the model employed and the success of RSM in optimizing the conditions of photocatalysis.

Keywords: *Reactive Red 120*; TiO_2; Photocatalysis; Response surface methodology (RSM); Central composite design (CCD); Canonical and ridge analyses

1. Introduction

Azo dyes, containing one or more azo bond (−N═N−), account for 60−70% of all textile dyestuffs used [1]. Other functional groups characterizing this class of compounds are also the auxochromes such as $-NH_2$, −OH, −COOH, $-SO_3H$ which are responsible for the increase of the color intensity and of the affinity with the fibers [2]. It is estimated that about 10−15% of the total production of colorants is lost during their synthesis and dyeing processes [3]. Reactive dyes exhibit a wide range of different chemical structures, primarily based on substituted aromatic and heterocyclic groups. Since reactive dyes are highly soluble in water, their removal from wastewater is difficult by conventional coagulation and the activated sludge processes [4–6]. AOPs were based on the generation of very reactive species such as hydroxyl radicals ($OH^{\bullet}$) that oxidize a broad range of pollutants quickly and non-selectively. Decolorization of azo reactive dyes by AOPs (O_3/UV [7], H_2O_2/UV [8], Fe^{2+}/H_2O_2 [9], TiO_2/UV [10]) has been described by several authors. Response surface methodology (RSM), an experimental strategy for seeking the optimum conditions for a multivariable system, is an efficient technique for optimization. Recently, it has been successfully applied to a different process for achieving its optimization

* Corresponding author. Tel.: +82 2 740 8891; fax: +82 2 745 9104.
E-mail address: zohkd@snu.ac.kr (K.-D. Zoh).

0143-7208/$ - see front matter © 2006 Elsevier Ltd. All rights reserved.
doi:10.1016/j.dyepig.2006.06.041

using experimental designs, which include TiO_2-coated/UV oxidation [11,12], TiO_2 slurry/UV oxidation [13,14], O_3 oxidation [15] and electrochemical oxidation [16]. However, the efficiency of treatment and the effect of interaction of various parameters using experimental design methodology during AOP processes have not been reported.

In this work, the TiO_2/UV process was applied on the commercially available azo reactive dye C.I. *Reactive Red 120*. A full factorial design (2^3) using the experimental design methodology was employed for the optimization of degradation conditions (measured by color and, TOC reduction of azo reactive dye) so that the main effects and interactions among variables can be estimated by keeping to a minimum the number of experiments.

2. Experimental design and central composite design (CCD)

To find the optimum conditions for degradation of the reactive dye in a circular type reactor, the experimental design as a function of the selected main factors has to be determined. As shown in Fig. 1, this rotatable experimental plan was carried out as a central composite design (CCD) consisting of 20 experiments. For three variables ($n = 3$) and two levels (low (−) and high (+)), the total number of experiments was 20 determined by the expression: 2^n ($2^3 = 8$: factor points) + $2n$ ($2 \times 3 = 6$: axial points) + 6 (center points: six replications), as shown in Tables 1 and 2.

The factors (variables) in this experiment were the dye concentration (X_1), TiO_2 concentration (X_2) and light intensity (X_3). A full second-order polynomial model obtained by multiple regression technique for three factors by using the SAS package (SAS Institute, Cary, NC, USA) and MINITAB package (Minitab Institute, USA) was adopted to describe the response surface. In developing the regression equation

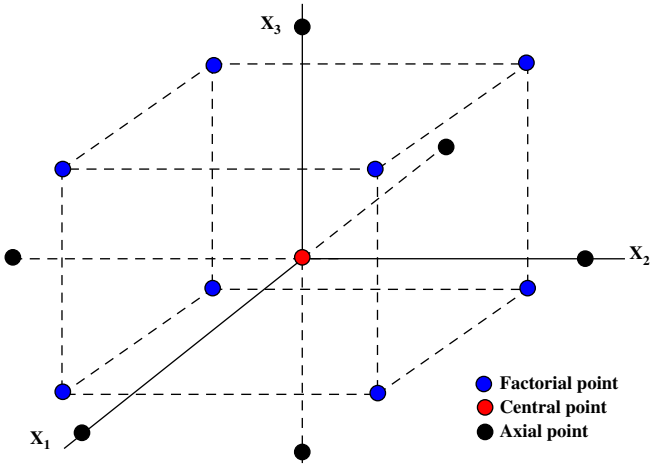

Fig. 1. Schematic diagram of central composite design (CCD) as a function of X_1 (TiO_2 concentration), X_2 (dye concentration), and X_3 (UV intensity) according to the 2^3 factorial design with six axial points and six central points (replication) (fixed factors: pH = 5, total volume = 3 L, flow rate = 1 L min^{-1}).

Table 1
The original and coded levels of the input variables

Original factors	Coded levels				
	−2	−1	0	1	+2
TiO_2 concentration ($g\,L^{-1}$): X_1	0.5	1	1.5	2	2.5
Dye concentration ($mg\,L^{-1}$): X_2	25	50	75	100	125
UV intensity ($mW\,cm^{-2}$): X_3	0	3	6	9	12

developed by Box–Hunter [17], the test factors were coded according to the following equation:

$$x_i = \frac{X_i - X_{io}}{\Delta X_i} \tag{1}$$

where x_i is the coded value of the ith independent variable, X_i the natural value of the ith independent variable, X_{io} the natural value of the ith independent variable at the center point, and ΔX_i is the step change value.

$$Y = b_0 + \sum_{i=1}^{k} b_i x_i + \sum_{i=1}^{k-1} \sum_{j=2}^{k} b_{ij} x_i x_j + \sum_{i=1}^{k} b_{ii} x_i^2 + e \tag{2}$$

where Y is the predicted response, b_0 and the offset term, b_i the linear effect, b_{ij} the squared effect and b_{ii} is the interaction effect. The three significant independent variables X_1, X_2, and X_3 and the mathematical relationship of the response Y

Table 2
The 2^3 factorial and central composite design for experiment

Experiment run	Pattern	Block	Variables in coded levels			Comment
			X_1	X_2	X_3	
1	− − −	1	−1	−1	−1	Full factorial
2	− + +		−1	+1	+1	Full factorial
3	+ − +		+1	−1	+1	Full factorial
4	+ + −		+1	+1	−1	Full factorial
5	0 0 0		0	0	0	Center − full factorial
6	0 0 0		0	0	0	Center − full factorial
7	− − +	2	−1	−1	+1	Full factorial
8	− + −		−1	+1	−1	Full factorial
9	+ − −		+1	−1	−1	Full factorial
10	+ + +		+1	+1	+1	Full factorial
11	0 0 0		0	0	0	Center − full factorial
12	0 0 0		0	0	0	Center − full factorial
13	−0 0	3	−2	0	0	Axial
14	+0 0		+2	0	0	Axial
15	0 − 0		0	−2	0	Axial
16	0 + 0		0	+2	0	Axial
17	0 0 −		0	0	−2	Axial
18	0 0 +		0	0	+2	Axial
19	0 0 0		0	0	0	Center − axial
20	0 0 0		0	0	0	Center − axial

on these variables can be approximated by quadratic/(second-degree) polynomial equation as shown below:

$$Y = b_0 + b_1X_1 + b_2X_2 + b_3X_3 + b_{11}X_1^2 + b_{22}X_2^2 + b_{33}X_3^2 + b_{12}X_1X_2 + b_{13}X_1X_3 + b_{23}X_2X_3 \quad (3)$$

where Y is the predicted response, b_0 the constant, b_1, b_2, and b_3 the linear coefficients, b_{12}, b_{13}, and b_{23} the cross-product coefficients, and b_{11}, b_{22}, and b_{33} are the quadratic coefficients.

3. Materials and methods

3.1. Materials

The molecular formula of *Reactive Red 120* (Ewha Chemicals Co., Ltd) with purity of >85% used in this study is shown in Table 3. Standard dye solution was prepared with a concentration of 50 mg L^{-1}, and λ_{max} was determined with a UV-spectrophotometer (Shimadzu UV-1201). Titanium dioxide used was anatase (Aldrich, 99.9+%). pH adjustments were conducted with 0.1 M H_2SO_4 and 0.1 M NaOH. All other chemicals were of analytical grades.

3.2. Photoreactor system and analysis

The entire experimental setup is shown in Fig. 2. All the experiments were carried out in a continuous flow through eight columns (each 10 mm in diameter) with a recirculation of the suspension. The UV lamps used in this study were 40 W blacklight blue fluorescent lamps (General Electrics Co., F40BLB, 1200-mm length, 32.5-mm diameter) with maximum emission at 254 nm. UV intensity was measured with a VLX-3W radiometer (Cole Parmer), which measures UV radiation at 254 nm. The effective volume of photoreactor was 1.88 L (550 mm (wide) × 640 mm (length) × 110 mm (height)). During operation, the photoreactor was wrapped in an aluminum foil to avoid any illumination by ambient light. The samples obtained from the photocatalytic reactions were analyzed by UV–vis spectroscopy (Shimadzu UV-1201), absorption at λ_{max} was 530 nm for azo dye of *Reactive Red 120*. TOC of photoreaction solution was measured by a TOC analyzer (Shimadzu, TOC500).

4. Results and discussions

4.1. The absorption spectrum and photocatalytic discoloration of Reactive Red 120 (RR120)

The temporal absorption spectral changes during the photocatalytic degradation of *Reactive Red 120* in illuminated aqueous TiO_2 suspensions are displayed in Fig. 3. The UV–vis absorption of *Reactive Red 120* is characterized by one band in the visible region, with its maxima located at 530 nm and by three bands at 215, 240, and 290 nm. These different peaks are attributed to the benzene and naphthalene rings substituted with SO_3^- and OH groups. The subsequent illumination of the aqueous *Reactive Red 120* causes continuous decrease of the intensities of UV and vis bands of *Reactive Red 120* with increasing irradiation time, which is not accompanied by the appearance of new absorption bands in the UV–vis region.

4.2. Photocatalytic kinetics on the effect of pH for decolorization of RR120

The experiments were carried out with a dye concentration of 50 mg L^{-1} at pH 3, 5, 7, 9 and 11 for 90 min. The wastewater from dye industries usually has a wide range of pH values. pH plays an important role both in the characteristics of dye wastes and in the generation of hydroxyl radicals. Hence, the effect of pH in the degradation of dyes by UV irradiation was investigated. The interpretation of pH effect on the efficiency of the photodegradation process is a difficult task since three possible reaction mechanisms can contribute to dye degradation, namely, hydroxyl radical attack, direct oxidation by the positive hole, and direct reduction by the electron in the conducting band.

According to the literature reports [18,19], the pH of the solution significantly affects TiO_2 activity, including the charge on the particles, the size of the aggregates it forms and the positions of the conductance and valence bands. pH changes can thus influence the adsorption of dye molecules onto the TiO_2

Table 3
Chemical structure of dyes and the properties of *Reactive Red 120*

Chemical structure	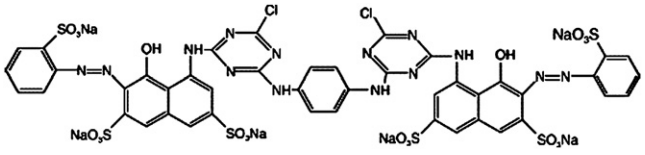
Molecular formula	$C_{44}H_{24}Cl_2N_{14}Na_6O_{20}S_6$
Molecular weight	1470 g mol^{-1}
Water solubility	70 g L^{-1}
Class	Diazo (–N=N– bond)

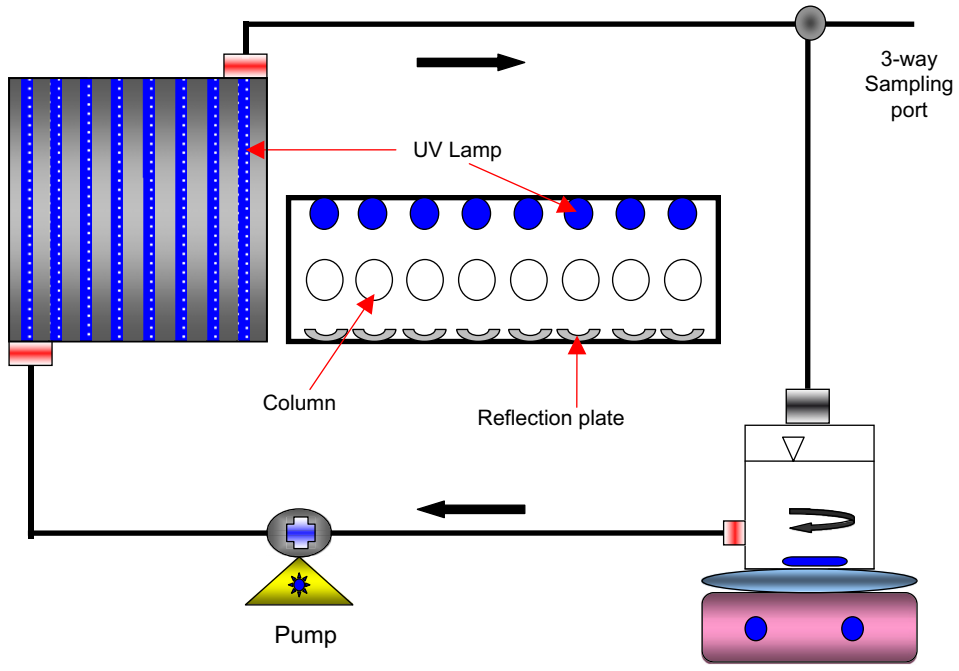

Fig. 2. Schematic diagram of the circular type photocatalytic reactor system.

surfaces, an important step for the photocatalytic oxidation to take place [20].

$$TiOH + H^+ \leftrightarrow TiOH_2^+ \quad (4)$$

$$TiOH + OH^- \leftrightarrow TiO^- + H_2O \quad (5)$$

The point of zero charge (pzc) of the TiO_2 (Degussa P25) is at pH 6.8 [21,22]. Thus, the TiO_2 surface is positively charged in acidic media (pH < 6.8), whereas it is negatively charged under alkaline conditions (pH > 6.8) [22,23]. Since R has three sulfonic groups in its structure, which is negatively charged, the acidic solution favors adsorption of dye onto the photocatalyst surface, thus k_{obs} increases as shown in Fig. 4 and Table 4. Thus, decolorization efficiency increased. At this pH, there is also the formation of OH• radicals, which react with dye molecules and increase the decolorization level. As the pH of the solution increased, the adsorption of dye molecules onto the catalyst surface decreased. Therefore, decolorization level was observed to be low at basic pH. Similar results have been reported for the photocatalytic oxidation of other azo dyes [24,25]. However, the photocatalytic degradation rate at alkaline pH was faster than that of at neutral pH.

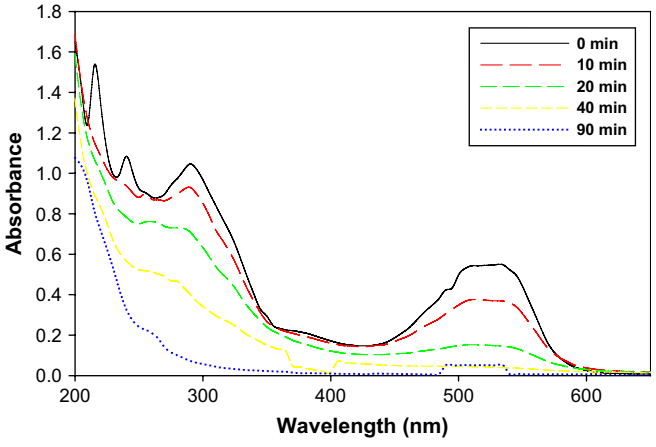

Fig. 3. UV–vis absorption spectrum of *Reactive Red 120* (*RR120*) at different irradiation times (experimental conditions: pH = 5, TiO_2 = 2 g L^{-1}, dye concentration = 50 mg L^{-1}, UV intensity = 9 mW cm^{-2}, total volume = 3 L, flow rate = 1 L min^{-1}).

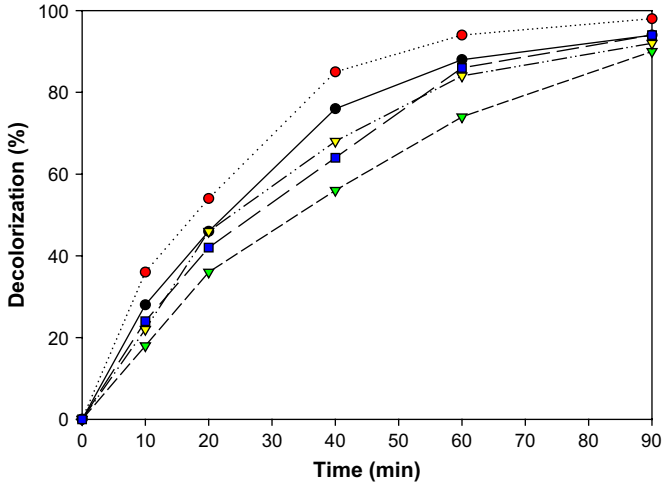

Fig. 4. Effect of initial pH on the photocatalytic oxidation of azo dye (*Reactive Red 120*) (experimental conditions: TiO_2 = 2 g L^{-1}, dye concentration = 50 mg L^{-1}, UV intensity = 9 mW cm^{-2}, total volume = 3 L, flow rate = 1 L min^{-1}).

Table 4
Apparent first-order rate constant k_{obs}, half-life $t_{1/2}$, and correlation coefficients R^2 for degradation of *Reactive Red 120* (50 ppm) at different pH

Azo dye	pH	k_{obs} (min^{-1})	$t_{1/2}$ (min)	R^2
Reactive Red 120	3	0.0323	21.46	0.991
	5	0.0448	15.47	0.995
	7	0.0240	31.22	0.990
	9	0.0319	21.72	0.991
	11	0.0287	21.15	0.990

4.3. The second-order model and analysis of variance (ANOVA)

All 20 experimental runs of central composite design (CCD) were performed in accordance with Table 2. As shown in Table 5, central composite design is composed of three independent variables X (TiO_2 concentration (X_1), dye concentration (X_2), and UV intensity (X_3)), and the response Y (% of color removal (Y_1), and % of TOC removal (Y_2)). The regression equations given in Table 6 were obtained from the analysis of variances.

Using 10, 5, and 1% significance levels, a model is considered significant if the p-value (significance probability value) is less than 0.1, 0.05, and 0.001, respectively. From the p-values presented in Table 7, it can be concluded that for two responses (Y_1, Y_2), linear contribution and quadratic contribution of the model were significant, whereas for the responses Y_1 and Y_2, cross-product contribution of the model was insignificant.

Actual (observed) value versus predicted value displays the real responses' data plotted against the predicted responses and are shown in Fig. 5(a) and (b). It is observed that there are tendencies in the linear regression fit, and the model explains the experimental range studied adequately. The fitted regression equation showed a good fit of the model.

Table 6
Regression equations obtained for color (Y_1) and TOC (Y_2) removal (%) of *RR120*

Regression equations
Analysis in coded factor (x_1, x_2, x_3)
$Y_1\ (\%) = 76.09 + 10.0x_1 - 15.75x_2 + 20.25x_3 + 3.18x_1^2 + 1.68x_2^2 - 15.32x_3^2 + 60x_1x_2 - 1.78x_1x_3 - 16x_2x_3$
$Y_2\ (\%) = 48.09 + 12.0x_1 - 16.0x_2 + 26.0x_3 - 12.82x_1^2 - 3.32x_2^2 - 17.32x_3^2 - 3.0x_1x_2 - 1.0x_1x_3 + 10.0x_2x_3$
Analysis in uncoded factor (X_1, X_2, X_3)
$Y_1\ (\%) = 69.84 - 8.55X_1 - 0.82X_2 + 12.48X_3 + 3.18X_1^2 + 0.004X_2^2 - 0.43X_3^2 + 0.12X_1X_2 + 0.0001X_1X_3 - 0.05X_2X_3$
$Y_2\ (\%) = -15.78 + 53.96X_1 - 0.23X_2 + 7.36X_3 - 12.82X_1^2 - 0.0013X_2^2 - 0.48X_3^2 - 0.06X_1X_2 + 0.167X_1X_3 + 0.003X_2X_3$

4.4. Estimation of quantitative effects of the factors

For estimation of the quantitative effects of the factors, Student's t-test was then performed. In Table 8, the factor effects of the model and associated p-values for the two responses are presented. A positive sign indicates a synergistic effect, while a negative sign represents an antagonistic effect of the factor on the selected response.

As shown in Table 8, the responses of Y_1 (% of color removal at 90 min) were significantly affected by the synergistic effect of linear term of UV intensity (X_3), with a p-value of

Table 5
Experimental values for color and TOC removal of *Reactive Red 120* after 90 min

Trial no.	Variables in uncoded levels						
	X_1	X_2	X_3	Y_1		Y_2	
	TiO_2 concentration	Dye concentration	UV intensity	Color removal (%)		TOC removal (%)	
				Actual value	Predicted value	Actual value	Predicted value
1	1	50	3	77	69.6	32	30.6
2	2	100	3	76	71.8	22	21.1
3	2	50	9	99	104.8	59	65.1
4	1	100	9	72	71.1	45	41.6
5	1.5	75	6	76	77.9	48	47.8
6	1.5	75	6	73	77.9	48	47.8
7	2	50	3	77	75.4	41	44.3
8	1	100	3	66	57.6	18	11.8
9	1	50	9	95	96.6	51	51.8
10	2	100	9	78	82.9	52	53.3
11	1.5	75	6	75	79.7	48	48.5
12	1.5	75	6	75	79.7	48	48.5
13	0.5	75	6	60	66.3	18	23.1
14	2.5	75	6	90	86.3	52	47.1
15	1.5	25	6	100	99.5	65	60.6
16	1.5	125	6	65	98.0	24	28.6
17	1.5	75	0	28	37.5	2	4.6
18	1.5	75	12	85	78.0	59	56.6
19	1.5	75	6	75	70.1	48	47.8
20	1.5	75	6	74	70.1	48	47.8

Table 7
Analysis of variance for two responses (Y_1, Y_2)

Source of variation	Responses			
	Y_1		Y_2	
	F value	p-value	F value	p-value
Model	21.45	0.0036***	26.43	<0.0001***
Linear contribution	6.23	0.0005***	68.61	<0.0001***
Quadratic contribution	7.31	0.0541*	9.80	0.0025**
Cross-product contribution	0.71	0.5566	0.88	0.4853

*Significant at 10% (p-value); **significant at 5% (p-value); and ***significant at 1% (p-value).

0.023, and the antagonistic effect of quadratic term of UV intensity (X_3^2) (p-value of 0.040). Table 8 also showed that the effect of the initial TiO_2 concentration (X_1), and reactive dye (X_2) was less pronounced than UV intensity (mW cm^{-2}), however the favorable quadratic effect (X_3^2) indicates that % degradation is improved at very low value. Finally, the most significant effect of first-order (linear term) derives from the initial intensity of UV (X_3).

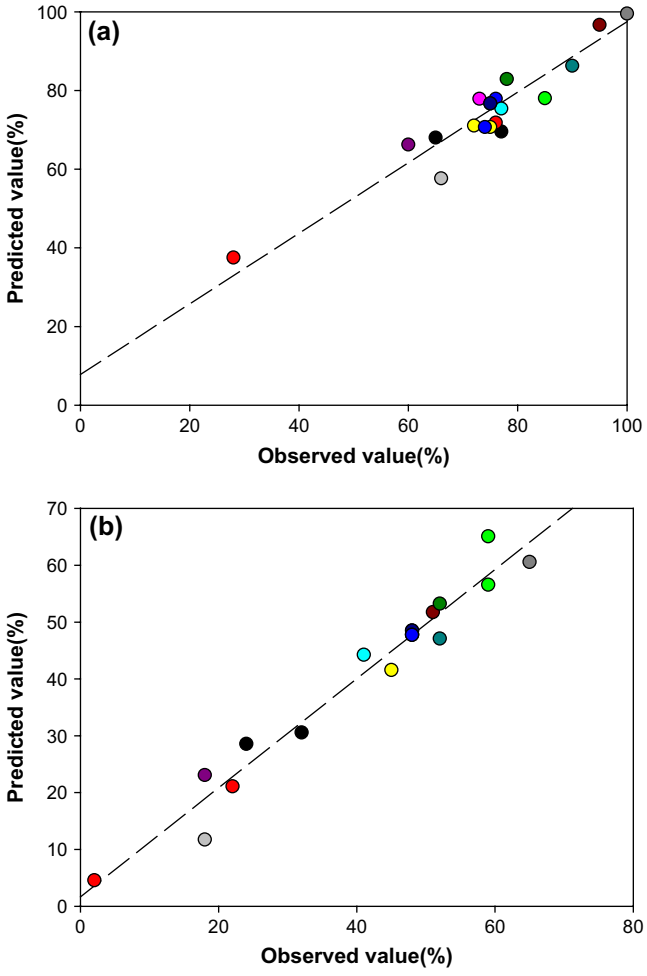

Fig. 5. The observed values (%) plotted against the predicted values (%) derived from the model of color (Y_1) and TOC (Y_2) removal (%) in uncoded values for $t = 90$ min. The long dash line is the regression line with regression coefficient $R = 0.90$ (a) and 0.96 (b). Each point refers to the experiment number listed in Table 5.

Significant factors for the responses Y_2 were linear terms of the TiO_2 (X_1), UV intensity (X_3), with p-values of 0.019 and 0.037, respectively. All above-mentioned factors show synergistic effect in the increase of TOC removal (%) of *Reactive Red 120*. Additionally, the quadratic terms of TiO_2 (X_1^2) and UV intensity (X_3^2) have an antagonistic effect on Y_2 responses (p-values of 0.016 and 0.003, respectively). Although the first-order effect shows that increases in both variables, TiO_2 (X_1) and UV intensity (X_3), favor TOC removal (%), an antagonistic effect was also observed between these two parameters. The simultaneous increase of TiO_2 (X_1^2) and UV intensity (X_3^2) is adverse for the reaction, as shown by the second-order effect (pure quadratic) of the last term in the polynomial expression.

4.5. Main and interaction effect plots

The main effect (mean) plot is appropriate for analyzing data in a designed experiment, with respect to important factors, where the factors are at two or more levels. Fig. 6(a) and 6(b) show the main effect plots of three variables (factors) on % of color and TOC removal, respectively. The application of the main effect (mean) plot to the defective springs data set results in the following conclusions:

Ranked list of factors (excluding interactions)

- Qualitatively, factor X_3 is the most important with difference between the two points, of approximately 56 and 57% in Y_1 and Y_2, respectively.
- Qualitatively, factor X_2 is the second most important to X_3 in Y_1 and Y_2.
- Qualitatively, factor X_1 is the third most important to X_3 in Y_1 and Y_2.

Increasing the concentration of TiO_2 can enhance the production of these species and leads to the greater removal of target organics. The results indicate that the increase in the TiO_2 concentration is associated with increase in the % of decolorization and TOC removal as shown in Fig. 6(a) and 6(b), respectively.

However, initial slopes of the curve increase greatly by increasing the catalyst loading from 0.5 to 1 g L^{-1}, above which initial slopes are nearly equal. At lower loading levels, such as 0.5 g L^{-1}, the catalyst surface and absorption of light by the catalyst surface are the limiting factors, and an increase in

Table 8
Factor effects and associated p-values for two responses

Relationship		Factor	Responses			
			Y_1		Y_2	
			Factor effect	p-value	Factor effect	p-value
Main effects	Linear	X_1	−0.30	0.773	2.945	0.019**
	Linear	X_2	−1.42	0.187	−0.661	0.527
	Linear	X_3	2.67	0.023**	2.496	0.037**
Interactions	Pure quadratic	X_1^2	0.49	0.640	−3.050	0.016**
		X_2^2	1.64	0.140	−0.762	0.468
		X_3^2	−2.35	0.040**	−4.133	0.003*
	Cross product	$X_1 \times X_2$	0.52	0.614	−0.417	0.688
		$X_2 \times X_3$	−1.39	0.196	0.139	0.893
		$X_1 \times X_3$	0.00	1.000	1.390	0.202

*Significant at 10% (p-value); **significant at 5% (p-value); and ***significant at 1% (p-value).
(+) Synergistic effect (factor effect).
(−) Antagonistic effect (factor effect).

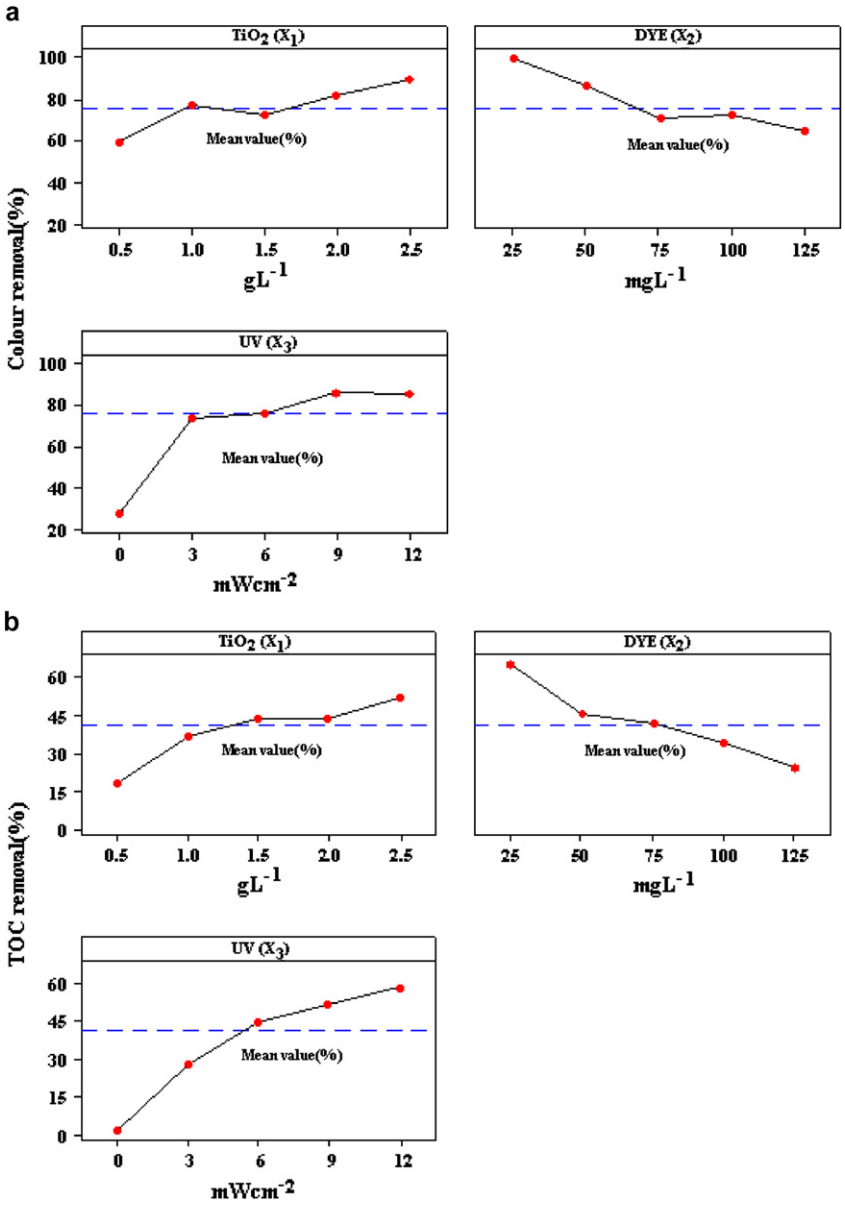

Fig. 6. Main effect plots for color (a) and TOC (b) removal (%) in uncoded value for $t = 90$ min.

catalyst loading greatly enhances the process efficiency. On the other hand, at higher loading levels, irradiation field inside the reaction medium is leveled off due to the light scattering by catalyst particles [26,27].

As seen in Fig. 6(a) and (b), the removal efficiency of color is inversely affected by the dye concentration. This negative effect can be explained as follows: as the dye concentration increases, the equilibrium adsorption of the dye onto the TiO_2 surface active sites increases, hence competitive adsorption of OH^- on the same sites decreases, resulting in the lower formation rate of $OH^{\bullet}$ radical which is the principal oxidant indispensable for the high degradation efficiency [28,29].

Also, the results (Fig. 6(a)) on the UV intensity are similar to TiO_2 concentration where the efficiency of the photo-oxidation reaction increased linearly with UV intensity up to a point, beyond which no further increases were observed. It is possible that the TiO_2 surface was fully utilized at 9 mW cm^{-2} of UV and the excitation of electron–hole pair by UV irradiation was a maximum at that point [30,31]. If so, further increases in UV intensity would have no additional effect on the rate of production of OH• radical.

In addition to the effect of each of the variables such as TiO_2 concentration, UV intensity, and dye concentration on the removal of dye individually, it is also important to check the interaction effect of these variables, especially two-factors interaction effect. Interaction plots were constructed by plotting both variables together on the same graph, and are shown in Fig. 7(a) and (b). This plot indicates that the most significant factor is UV intensity (X_3) in Y_1 and Y_2 and the most significant interaction is between TiO_2 (X_1) and UV intensity (X_3).

As can be seen in Fig. 7(a), the highest % of decolorization is reached at TiO_2 (1.5 g L^{-1}) and 12 mW cm^{-2} of UV intensity at dye concentration (75 mg L^{-1}) in line of interaction effect between TiO_2 (X_1) and UV intensity (X_3). The interaction of TiO_2 (1.5 g L^{-1})/UV intensity (0 mW cm^{-2}) in the absence of UV illumination at reactive dye (75 mg L^{-1}), however, presented very low efficiency of the color removal (%). Run 17 in the dark condition (TiO_2 alone) as shown in Table 5 showed approximately 28% of decolorization after 90 min, but no by-product was produced. This result indicates that a portion of reactive dye was not degraded, but rather adsorbed onto the TiO_2 particles. For the highest % of TOC removal in Y_2, Fig. 7(b) showed that the response was quite similar to Y_1 response. As mentioned, the most favorable TOC removal (%) for Y_2 was obtained by TiO_2 (1.5 g L^{-1}) − 12 mW cm^{-2} of UV intensity at dye concentration (75 mg L^{-1}) in line of interaction effect between TiO_2 (X_1) and UV intensity (X_3). Compared to the factors interaction between of TiO_2 (X_1) and UV intensity (X_3), however, the dye concentration (X_2) and UV intensity (X_3) were considerably higher in the % of decolorization and TOC removal. Thus, qualitatively, the interaction effect between dye concentration (X_2) and UV intensity (X_3) is the second most important to between TiO_2 (X_1) and UV intensity (X_3).

4.6. Response surface (contour) plots and optimization conditions

Canonical analysis using SAS package is a mathematical approach to examine the overall shape of the curve, to locate the stationary point of the response surface, and to decide whether it describes a maximum, minimum, or saddle point. Three-dimensional (3D) and contour (2D) plots for the predicted responses were also formed, based on the model polynomial functions to assess the change of the response surface as shown in Figs. 8 and 9. The relationship between the dependent (Y_1, Y_2) and independent variables (X_1, X_2, X_3) can be also further understood by these plots. Since the model has more than two factors, one factor was held constant for each diagram; therefore, a total of six response surface diagrams were produced for each response (Y_1, Y_2). Fig. 8(a) describing the minimum point for Y_1 response shows graphical 3D and 2D representations of the polynomial obtained from the matrix. As shown in Fig. 8(b), the stationary point of the response surface shows the saddle point. The responses' surface and contour plots showing effect of dye and UV intensity on the % of decolorization have saddle behavior as shown in Fig. 8(c).

Next, the effects of TiO_2 (X_1) and dye (X_2) concentrations, while keeping UV intensity (X_3) at the middle level (6 mW cm^{-2}), are shown in Fig. 9(a). As shown in Fig. 9(a), the increase in TiO_2 concentration (X_1) and the decrease in UV intensity (X_3) increased in % of TOC removal at the ranges of TiO_2 concentration (2 g L^{-1}) and dye concentration of less than 50 mg L^{-1} described as the saddle point for Y_2 response.

The effect of dye concentration (X_2) and UV intensity (X_3) at the middle TiO_2 concentration (X_1) of 1.5 g L^{-1} is also shown in Fig. 9(b) which described as the maximum point for Y_2 response. This contour plot indicates a wide range of TOC removal (%) combinations resulting in a low dye concentration. On the contrary, working at low UV intensity values, the quantity of dye concentration added did not significantly affect the % of TOC removal.

The resulting response surface and contour plots is shown in Fig. 9(c). This result demonstrates that the response surface has a maximum point. Therefore, several optima could be found depending on the UV intensity. On the other hand, the influence of UV intensity on the % of TOC removal was dependent on the TiO_2 concentration. The stationary points (maximum, minimum, and saddle points) were obtained by canonical analysis and the response surface around these stationary points was evaluated. Also, the coordinates of local minima in terms of the processing variables were determined by differentiating Eq. (6) for TiO_2 concentration, Eq. (7) for dye concentration, and Eq. (8) for UV intensity to X_1, X_2, X_3, and setting the result thus obtained equal to zero, according to the following equations [32]:

$$\left[\frac{\partial t_{TiO_2}}{\partial X_1}\right]_{X_2,X_3} = 0 \tag{6}$$

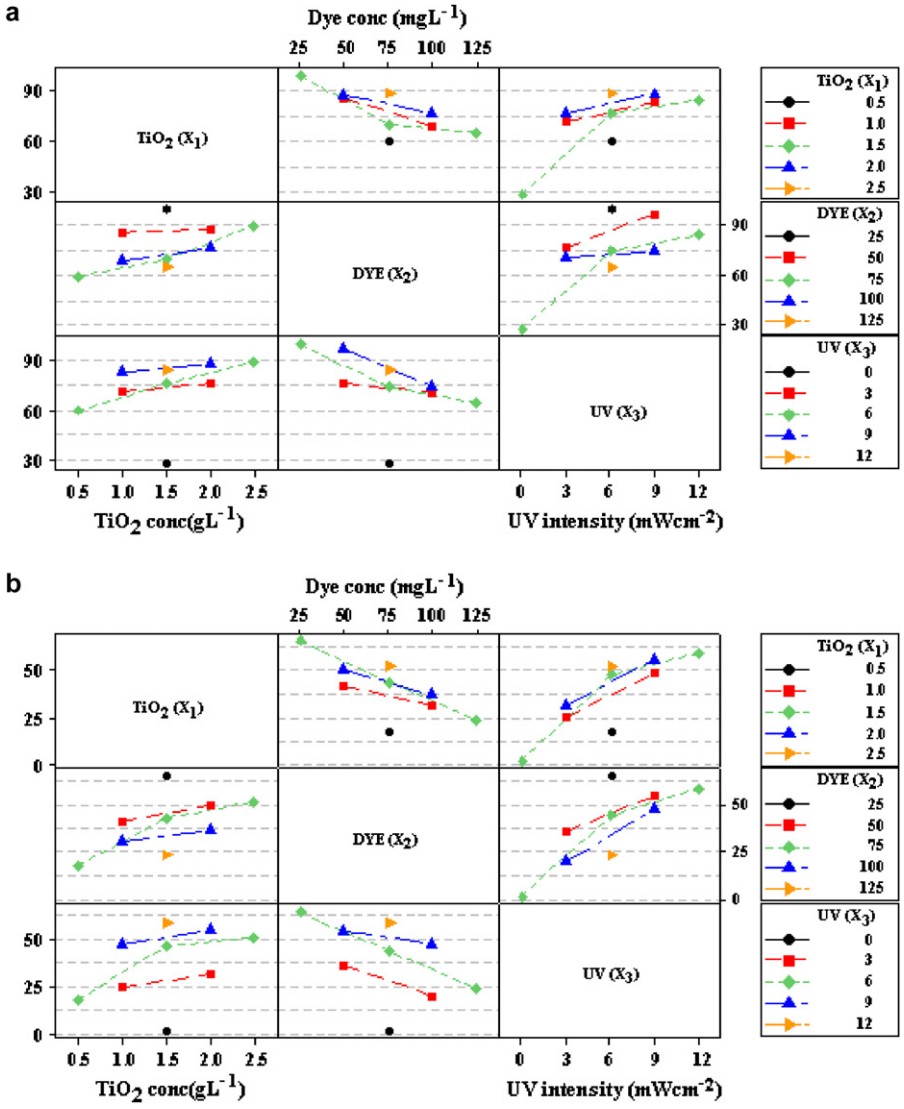

Fig. 7. Two-way interaction plots for color (a) and TOC (b) removal (%) in uncoded values for $t = 90$ min.

$$\left[\frac{\partial t_{\mathrm{Dye}}}{\partial X_2}\right]_{X_1,X_3} = 0 \tag{7}$$

$$\left[\frac{\partial t_{\mathrm{UV}}}{\partial X_3}\right]_{X_1,X_2} = 0 \tag{8}$$

The conditions obtained at the saddle point for total Y_1 responses were $X_1 = 1.63\ \mathrm{g\,L^{-1}}$, $X_2 = 45.2\ \mathrm{mg\,L^{-1}}$ and $X_3 = 8.1\ \mathrm{mW\,cm^{-2}}$, and the conditions at maximum point for total Y_2 responses were $X_1 = 1.92\ \mathrm{g\,L^{-1}}$, $X_2 = 34.7\ \mathrm{mg\,L^{-1}}$ and $X_3 = 8.5\ \mathrm{mW\,cm^{-2}}$. These points were located within the experimental ranges, implying that the analytical techniques could be used to identify the minimum condition. The principal effects of processing variables appear to be unidirectional; however, at certain conditions, comparing with TOC characteristics, the decolorization characteristics demonstrate conflicting interactions. In general, higher UV intensity and lower dye concentration favorably improved % of color and TOC removal. It may be necessary to make an acceptable compromise in all the response results. However, it should also be noted that the above general observations are only true for the regions bound by the stationary point.

4.7. Model validation and confirmation

Verification experiments performed at the predicted conditions derived by from ridge analysis of RSM demonstrated that the experimental values were reasonably close to the predicted values as shown in Table 9, indicating the validity and adequacy of the predicted models. Moreover, the verification experiments also proved that the predicted values of the % of decolorization and TOC removal could be achieved within 95% confidence interval of the experimental values.

5. Conclusions

The optimization and the modeling of photocatalytic degradation of azo dye (*Reactive Red 120*) were performed by using a composite experimental design. The ensuing mathematical

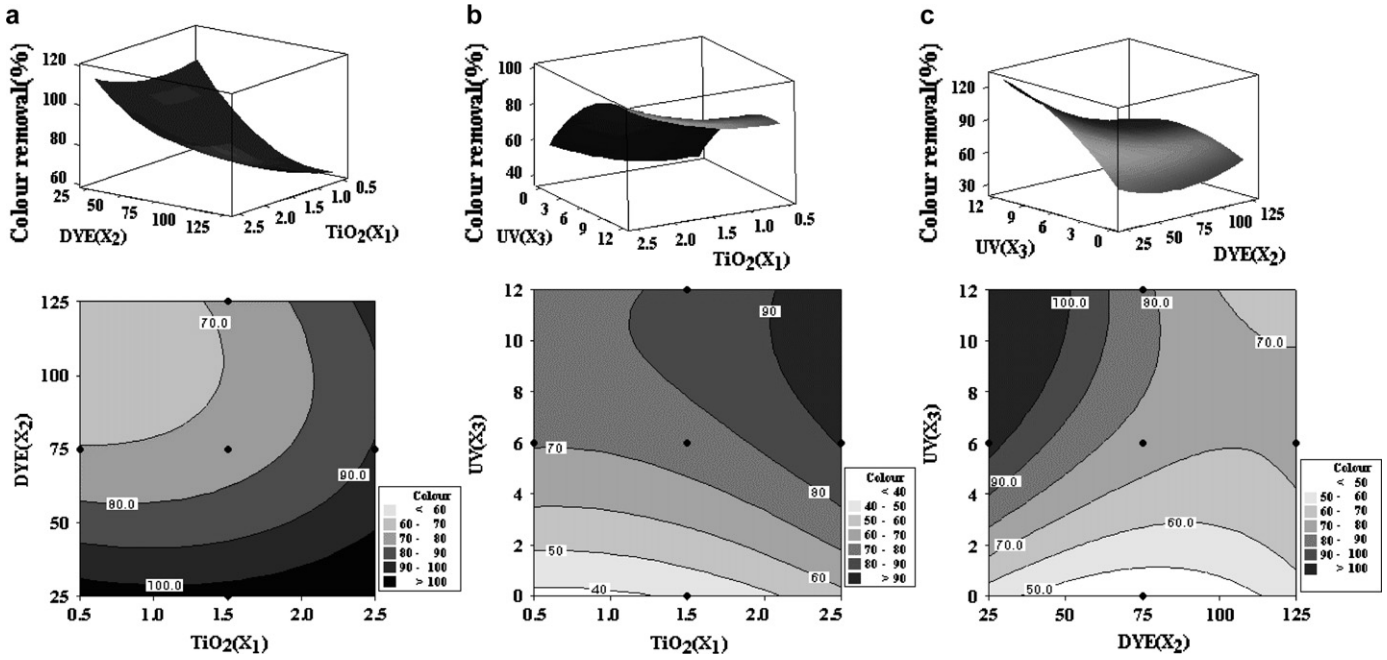

Fig. 8. Surface and contour plots of color removal (%) in uncoded values for $t = 90$ min. (a) X_1 (TiO_2) and X_2 (dye) in fixed X_3 (UV) at 6 mW cm^{-2}, (b) X_2 (dye) and X_3 (UV) in fixed X_1 (TiO_2) at 1.5 g L^{-1}, (c) X_1 (TiO_2) and X_3 (UV) in fixed X_2 (dye) at 75 mg L^{-1}.

model could predict the photocatalytic degradation at any point in the experimental domain as well as the determination of the optimal degradation conditions. Acidic and alkaline pH took less time (the half-time $t_{1/2}$) for complete decolourization compared with neutral pH. At neutral pH, the rate of azo dye (*RR120*) degradation is low in terms of decolorization compared with that at acidic and alkaline pH. The high correlation in the model indicates that the second-order polynomial model could be used to optimize the photocatalytic degradation of dye. The conditions to get 100% for Y_1 response of decolorization were found to be 1.63 g L^{-1} TiO_2 (X_1), 45.2 mg L^{-1} of reactive dye (X_2), and 8.1 mW cm^{-2} of UV intensity (X_3) and the conditions to get 67.27% for Y_2 response of TOC removal to were 1.92 g L^{-1} TiO_2 (X_1), 34.7 mg L^{-1} of reactive dye (X_2), and 8.5 mW cm^{-2} of UV intensity (X_3), respectively. Under optimized conditions, the experimental values agreed with

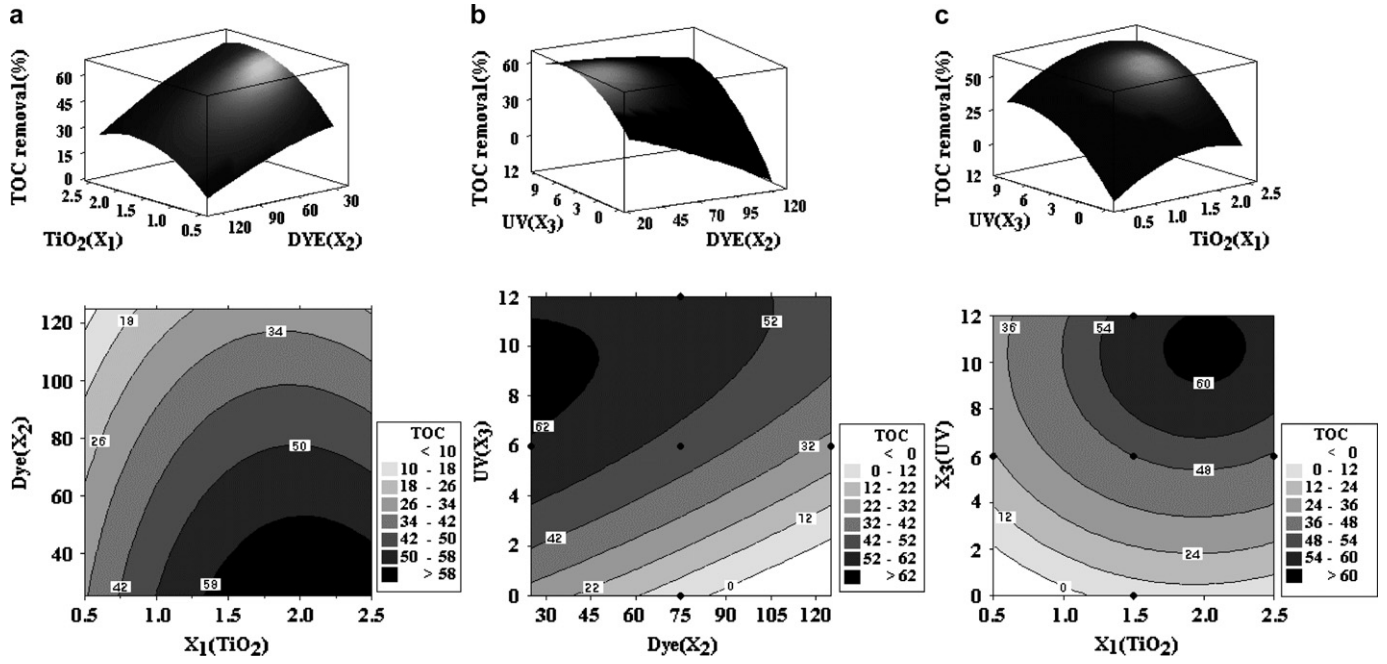

Fig. 9. Surface and contour plots of TOC removal (%) in uncoded values for $t = 90$ min. (a) X_1 (TiO_2) and X_2 (dye) in fixed X_3 (UV) at 6 mW cm^{-2}, (b) X_2 (dye) and X_3 (UV) in fixed X_1 (TiO_2) at 1.5 g L^{-1}, (c) X_1 (TiO_2) and X_3 (UV) in fixed X_2 (dye) at 75 mg L^{-1}.

Table 9
Comparison of experimental and predicted values of two responses (Y_1, Y_2) at the optimal levels predicted by RSM for additional experiments (three trials)

Response	Optimal conditions	Stationary point	Predicted value (%)[a]	Observed value (%)[b]
Y_1	$X_1 = 1.63\ g\ L^{-1}$, $X_2 = 45.2\ mg\ L^{-1}$, $X_3 = 8.1\ mW\ cm^{-2}$	Saddle	100	98 ± 2
Y_2	$X_1 = 1.92\ g\ L^{-1}$, $X_2 = 34.7\ mg\ L^{-1}$, $X_3 = 8.5\ mW\ cm^{-2}$	Maximum	67.3	66 ± 3

[a] Predicted using ridge analysis of response surface quadratic model.
[b] Mean ± standard deviation of triplicate determinations from different experiments.

the values predicted by the ridge analysis. These results implicate that the optimization using a response surface methodology based on the central composite design can save the time and effort by the estimation of the optimum conditions of the maximum removal of dye.

References

[1] Muruganandham M, Swaminathan M. Solar photocatalytic degradation of a reactive azo dye in TiO_2-suspension. Solar Energy Materials and Solar Cells 2004;81(4):439–57.
[2] Molinari R, Pirillo F, Falco M, Loddo V, Palmisano L. Photocatalytic degradation of dyes by using a membrane reactor. Chemical Engineering and Processing 2004;43(9):1103–14.
[3] Konstantinou IK, Albanis TA. TiO_2-assisted photocatalytic degradation of azo dyes in aqueous solution: kinetic and mechanistic investigations. A review. Applied Catalysis B: Environmental 2004;49(1):1–14.
[4] Tang C, Chen V. The photocatalytic degradation of reactive black 5 using TiO_2/UV in an annular photoreactor. Water Research 2004;38(11): 2775–81.
[5] Akyol A, Yatmaz HC, Bayramoglu M. Photocatalytic decolorization of Remazol Red RR in aqueous ZnO suspensions. Applied Catalysis B: Environmental 2004;54(1):19–24.
[6] Gouvêa CA, Wypych F, Moraes SG, Durán N, Nagata N, Peralta-Zamora P. Semiconductor-assisted photocatalytic degradation of reactive dyes in aqueous solution. Chemosphere 2000;40(4):433–40.
[7] Uygur A. An overview of oxidative and photooxidative decolorization treatments of textile waste waters. Journal of the Society of Dyers and Colourists 1997;113:211–7.
[8] Aplin R, Waite TD. Comparison of three advanced oxidation processes for degradation of textile dyes. Water Science and Technology 2000;42(5):345–54.
[9] Moraes SG, Freire RS, Duran N. Degradation and toxicity reduction of textile effluent by combined photocatalytic and ozonation processes. Chemosphere 2000;40(4):369–73.
[10] Masten SJ, Davies SHR. The use of ozonation to degrade organic contaminants in wastewaters. Water Science and Technology 1994;28(4):180–5.
[11] Danion A, Bordes C, Disdier J, Gauvrit JV, Guillard C, Lantéri P, et al. Optimization of a single TiO_2-coated optical fiber reactor using experimental design. Journal of Photochemistry and Photobiology A: Chemistry 2004;168(3):161–7.
[12] Fernández J, Kiwi J, Baeza J, Freer J, Lizama C, Mansilla HD. Orange II photocatalysis on immobilised TiO_2: effect of the pH and H_2O_2. Applied Catalysis B: Environmental 2004;48(3):205–11.
[13] Amat AM, Arques A, Bossmann SH, Braun A, Göb S, Miranda MA, et al. Oxidative degradation of 2,4-xylidine by photosensitization with 2,4,6-triphenylpyrylium: homogeneous and heterogeneous catalysis. Chemosphere 2004;57(9):1123–30.
[14] Lizama C, Freer J, Baeza J, Mansilla HD. Optimized photodegradation of Reactive Blue 19 on TiO_2 and ZnO suspensions. Catalysis Today 2002;76(2):235–46.
[15] Chen LC. Effects of factors and interacted factors on the optimal decolorization process of methyl orange by ozone. Water Research 2000;34(3):974–82.
[16] Gursesa A, Yalcina M, Dogarb C. Electrocoagulation of some reactive dyes: a statistical investigation of some electrochemical variables. Waste Management 2000;22:491–4.
[17] Box G, Hunter WG. Statistics for experimenters: an introduction to design, data analysis, and model building. Wiley; 1987.
[18] Neppolian B, Choi HC, Sakthivel S, Arabindoo B, Murugesan V. Solar/UV-induced photocatalytic degradation of three commercial textile dyes. Journal of Hazardous Materials 2002;89(2–3):303–17.
[19] Toor AP, Verma A, Jotshi CK, Bajpai PK, Singh V. Photocatalytic degradation of Direct Yellow 12 dye using UV/TiO_2 in a shallow pond slurry reactor. Dyes and Pigments 2006;68:53–60.
[20] Alaton IA, Balcioglu IA, Bahnemann DW. Advanced oxidation of a reactive dyebath effluent: comparison of O_3, H_2O_2/UV-C and TiO_2/UV-A processes. Water Research 2002;32:1143.
[21] Hasnat MA, Siddiquey A, Nuruddin A. Comparative photocatalytic studies of degradation of a cationic and an anionic dye. Dyes and Pigments 2005;66(3):185–8.
[22] Kusvuran E, Irmak S, Yavuz I, Samil A, Erbatur O. Comparison of the treatment methods efficiency for decolorization and mineralization of Reactive Black 5 azo dye. Journal of Hazardous Materials 2005; 119(1–3):109–16.
[23] Daneshvar N, Rabbani M, Modirshahla N, Behnajady MA. Kinetic modeling of photocatalytic degradation of Acid Red 27 in UV/TiO_2 process. Journal of Photochemistry and Photobiology A: Chemistry 2004;168(1–2):39–45.
[24] Kusvuran E, Gulnaz O, Irmak S, Atanur OM, Yavuz HI, Erbatur O. Comparison of several advanced oxidation processes for the decolorization of *Reactive Red 120* azo dye in aqueous solution. Journal of Hazardous Materials 2004;109(1–3):85–93.
[25] Tang WZ, An H. UV/TiO_2 photocatalytic oxidation of commercial dyes in aqueous solutions. Chemosphere 1995;31(9):4157–70.
[26] Son HS, Lee SJ, Cho IH, Zoh KD. Kinetics and mechanism of TNT degradation in TiO_2 photocatalysis. Chemosphere 2004;57(4): 309–17.
[27] Adesina AA. The photo-oxidative degradation of sodium dodecyl sulfate in aerated aqueous TiO_2 suspension. Journal of Photochemistry and Photobiology A: Chemistry 1998;118:111–22.
[28] Daneshvar N, Salari D, Khataee AR. Photocatalytic degradation of azo dye acid red 14 in water: investigation of the effect of operational parameters. Journal of Photochemistry and Photobiology A: Chemistry 2003;157(1):111–6.
[29] Tennakone K, Kiridena WCB, Punchihewa S. Photodegradation of visible-light-absorbing organic compounds in the presence of semiconductor catalysts. Journal of Photochemistry and Photobiology A: Chemistry 1992;68(3):389–93.
[30] Sakthivela S, Neppolianb B, Shankarb MV, Arabindoob B, Palanichamyb Mand, Murugesan V. Solar photocatalytic degradation of azo dye: comparison of photocatalytic efficiency of ZnO and TiO_2. Solar Energy Materials and Solar Cells 2003;77:65.
[31] Minero C, Maurino V, Pelizzetti E. Heterogeneous photocatalytic transformations of *s*-triazine derivatives. Research on Chemical Intermediates 1997;23:291–310.
[32] Pandey PK, Ramaswamy HS, St-Gelais D. Effect of high pressure processing on rennet coagulation properties of milk. Innovative Food Science and Emerging Technologies 2003;4(3):245–56.